Designing the 3/5 biorthogonal wavelet using factor multiplication approach for extracting the iris image features

R. Rizal Isnanto, Kodrat Iman Satoto, Ike Pertiwi Windasari
Lecturer and Researcher in Computer Engineering, Universitas Diponegoro, Jalan Prof. H. Soedarto, S.H., Semarang, Indonesia

Abstract

Designing the new wavelet should be done to find a most matched wavelet to extract the iris image features applied for recognition purposes. In this research, a new biorthogonal wavelet was designed based on Haar filter properties and Haar's orthogonality conditions. One approach is the use of factor multiplication in designing a biorthogonal wavelet. The 3/5 biorthogonal wavelet gives the better results than other types of wavelets, based on its mean-squared error (MSE) and Euclidean distance parameters, as well as based on recognition rate, to extract the iris image features.

Keywords: iris, 3/5 biorthogonal wavelet, factor multiplication approach, MSE, Euclidean distance.

1 Introduction

1.1 Background

Iris is the part of the circle around eye pupil. Although iris has a relatively narrow region compared with entire area of the human body, iris has a very unique and stable pattern.

Many algorithms have been applied as a method of iris recognition, such as principal component analysis, independent component analysis, Gabor-Wavelet algorithm, Gray Level Co-occurrence Matrix, and others. In constructing a biorthogonal wavelet used to extract iris features, a 5/7 filter type wavelet has

www.witpress.com, ISSN 1743-3517 (on-line)
doi:10.2495/Intelsys130271

been designed [7]. In this research, a new 3/5 biorthogonal wavelet will be developed using factor multiplication for extracting the iris image features.

1.2 Research objective

The purpose of making this research is to develop a new 3/5 biorthogonal wavelet (bior3.5). Some parameters in Haar filter properties and Haar's orthogonality conditions will be applied. The length of the filters are 3 (three) for decomposition and 5 (five) for reconstruction.

1.3 Limitation

The research has problem limitations as follows:

a. Iris image used is the image from database of CASIA V1.0—Portions of the research in this paper use the CASIA-IrisV1 collected by the Chinese Academy of Sciences' Institute of Automation (CASIA)—and iris images captured using Irdosoft 4.0 camera.
b. Research uses Haar filter parameters and its orthogonality properties as the basis for reconstructing a new 3/5 biorthogonal wavelet. Haar's parameters are used because it perform the best in recognizing iris images based on recognition rate [7] as well as based on energy compaction [4].
c. Test parameters used are mean-squared error (MSE), Euclidean distance parameters, and recognition rate.

2 Basis of theory

2.1 Iris eyes

Iris can serve as the basis for biometric systems. Each iris has a texture that is very detailed and unique to each person and remains stable for decades [4]. The eye cannot be altered through surgery without causing any damage to eyesight. Figure 1 shows the view of human eyes.

2.2 Wavelet transform

Wavelets are mathematical functions that satisfy certain requirements are able to perform the decomposition of a function [5]. Wavelet can be used to describe a model or the original image into a mathematical function regardless of the shape of the model in the form of a image, a curve, or a plane. Wavelet transform is a function that converts the signals from region to region the frequency or time scale. The most appropriate wavelet transform used in image processing because there is not much information is lost during the reconstruction.

Image processing using wavelet transform is done by filtering image using wavelet filter. Result of this filtering is four image subspaces from original image. These four subspaces are in wavelet domain. Four subspaces mentioned are lowpass–lowpass (LL), lowpass–highpass (LH), highpass–lowpass (HL), and

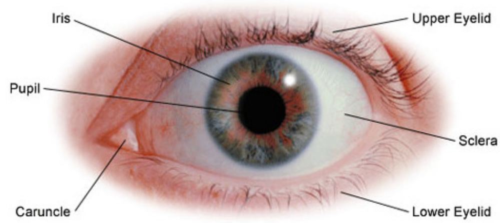

Figure 1: View of human eyes (courtesy of www.gcot.net).

highpass–highpass (HH). This process is called decomposition [4] which can be continued using LL as its input for getting next decomposition levels.

2.3 Normalized Euclidean distance

After passing through feature extraction process and parameter values are obtained, then the next stage is calculating the nearest distance (Euclidean distance) of feature vector values of an image [7]. The Euclidean distance between values of feature vectors (B) of input image (A) and values of feature vector of jth image can be expressed as:

$$D(A,B) = \sqrt{\sum_{i=0}^{n} \frac{\left(\left|A_i - B_i\right|\right)^2}{A_i}} \quad (1)$$

where $D(A, B)$ = Euclidean distance between iris A and B, A_i = Feature vector of iris A, B_i = Feature vector of iris B, n = vector length (sum of textural features) of vector A and vector B

2.4 Succesive approximation or cascade algorithm

One approach to calculate $\varphi(t)$ and $\psi(t)$ is a form of succesive approximation used theoretically to prove existence and uniqueness of $\varphi(t)$ and to actually calculate them. The basic recursion equation that comes from multiresolution formula is

$$\phi(t) = \sum_{n} h[n]\sqrt{2}\phi^{(k)}(2t-n) \quad (2)$$

where $h(n)$ is the scaling coefficients and $\varphi(t)$ is the scaling function. To solve the basic recursion of Eq. (2), an iterative algorithm that generates successive approximations to $\psi(t)$ is applied [2]. If the algorithm converges to a fixed point, this point is a solution to Eq. (2). The iteration is defined by

$$\phi^{(k+1)}(t) = \sum_{n=0}^{N-1} h[n]\sqrt{2}\phi^{(k)}(2t-n) \quad (3)$$

This iteration converges to $\varphi(t)$. From this $\varphi(t)$, then the wavelet function can be generated from

$$\psi(t) = \sum_{n=-\infty}^{\infty} g[n]\sqrt{2}\phi^{(k)}(2t-n) \tag{4}$$

Because it applies the same operation over and over to the output of the previous application, it is known as the *cascade algorithm* [13].

2.5 Biorthogonal wavelet

A biorthogonal wavelet is a wavelet where the associated wavelet transform is invertible but not necessarily orthogonal. Designing biorthogonal wavelets allow more degrees of freedom than orthogonal wavelets.

In the biorthogonal case, there are two scaling functions $\varphi, \tilde{\varphi}$, which may generate different multiresolution analyses, and accordingly two different wavelet functions $\psi, \tilde{\psi}$. So the numbers M and N of coefficients in the scaling sequences $a, \tilde{a}$ may differ. The scaling sequences must satisfy the following biorthogonality condition [5].

$$\sum_{n\in Z}^{\infty} a_n \tilde{a}_{n+2m} = 2.\delta_{m,0} \tag{5}$$

Then the wavelet sequences can be determined as

$$b_n = (-1)^n \tilde{a}_{M-1-n}, n = 0,\ldots,M-1 \tag{6}$$

$$\tilde{b}_n = (-1)^n a_{M-1-n}, n = 0,\ldots,N-1 \tag{7}$$

3 Design of research

In constructing a new 3/5 biorthogonal wavelet, some steps can be detailed as follows.

a. Deriving and obtaining equations for 3- and 5-tap filters which satisfies orthogonality conditions.
b. Determining the components of h and $\bar{h}$ for decomposition and reconstruction, respectively.
c. Testing the results of point b in case of its double-shift orthogonality.
d. Plotting and depicting two graphics both scaling function as well as wavelet function for decomposition purpose using cascade algorithm applied up to 20 iterations.

e. Plotting and depicting two graphics both scaling function as well as wavelet function for reconstruction purpose using cascade algorithm applied up to 20 iterations.
f. Testing the wavelet designed using both MSE and Euclidean distance measures between reconstructed iris images after decomposition and its original images.
g. Comparing both MSE and Euclidean distance (results from point f) against other types of wavelets which had ever observed (i.e., Haar, db5, coif3, sym4, and bior2.4).
h. Concluding some results of points f and g to give research conclusions.

The reasons why we choose 3/5 biorthogonal filter are biorthogonal wavelet bases maintain the symmetry for wavelets and scaling functions by relaxing the orthogonality constraint, while none of the orthogonal wavelet systems, except Haar, has symmetrical coefficients [3]. Also, in the orthogonal wavelets, filter and scaling filter must be of the same length, and the length must be even [2]. This restriction has been relaxed for biorthogonal filters. Since we had done some research previously to construct Biorthogonal 5/7 filter [7] to represent medium–medium length filter, then we choose Biorthogonal 3/5 as a representative of a relatively short-medium filters with odd lengths both for analysis and synthesis, respectively. The categorization of short–medium–long refers to the research to observe the relationship between the averaged SNR and the length of the filters when orthogonal wavelets – Daubechies' wavelets, symlets, and coiflets have been used. From that research, a maximum SNR is achieved for wavelets in which corresponding filter is with medium length [6]. Short filter range is 1–4, medium filter range is 5–12, and long filter range exceeds 12.

For example, we need 3/5 biorthogonal with symmetric scaling filters. The three-tap filter then can be written as a modified form which is stated by Soman *et al.* [3]:

$$h = \{h_{-1}, h_0, h_1\} = \left\{\frac{1}{2\sqrt{2}}, \frac{2}{2\sqrt{2}}, \frac{1}{2\sqrt{2}}\right\} = \left\{\frac{1}{2\sqrt{2}}, \frac{1}{\sqrt{2}}, \frac{1}{2\sqrt{2}}\right\} \tag{8}$$

These filters has symmetrical characteristics with sum of its components is √2, which matched with orthogonality requirements on wavelets. Then, when the second filters $\overline{h}$ is stated as:

$$\overline{h} = \{\overline{h}_{-2}, \overline{h}_{-1}, \overline{h}_0, \overline{h}_1, \overline{h}_2\} \tag{9}$$

To fulfill the orthogonality condition, $\overline{H}(z)\big|_{z=1} = \sum_k \overline{h}_k = \sqrt{2}$, also the equation $\overline{H}(z)\big|_{z=-1} = 0$ which is one requirement of low-pass filter (LPF), therefore $\overline{H}(z)$ can be written as [3].

$$\begin{array}{ccccc} \bullet & h_{-1} & h_0 & h_1 & \bullet \\ \bar{h}_{-2} & \bar{h}_{-1} & \bar{h}_0 & \bar{h}_1 & \bar{h}_2 \end{array}$$

Figure 2. First position of 3/5 filters.

$$\begin{array}{ccccc} \bullet & \bullet & \bullet & h_{-1} & h_0 \\ \bar{h}_{-2} & \bar{h}_{-1} & \bar{h}_0 & \bar{h}_1 & \bar{h}_2 \end{array}$$

Figure 3. Position of 3/5 filters after one double-shift.

$$\overline{H}(z) = \sqrt{2} z^{-1} \left(\frac{1+z}{2} \right)^2 \left(\frac{1-a}{2} z^{-1} + a + \frac{1-a}{2} z \right) \tag{10}$$

which obtains an LPF with filter length of 5. The first position of the filters can be depicted in Figure 2.

By expanding and simplifying (11) for $\overline{H}(z)$, we can get

$$\overline{H}(z) = \left(\frac{1-a}{4\sqrt{2}} \right) z^{-2} + \left(\frac{2}{4\sqrt{2}} \right) z^{-1} + \left(\frac{2+2a}{4\sqrt{2}} \right) + \left(\frac{2}{4\sqrt{2}} \right) z + \left(\frac{1-a}{4\sqrt{2}} \right) z^2 \tag{11}$$

$$\bar{h} = \left(\bar{h}_{-2}, \bar{h}_{-1}, \bar{h}_0, \bar{h}_1, \bar{h}_2 \right) = \left(\frac{1-a}{4\sqrt{2}}, \frac{1}{2\sqrt{2}}, \frac{1+a}{2\sqrt{2}}, \frac{1}{2\sqrt{2}}, \frac{1-a}{4\sqrt{2}} \right) \tag{12}$$

For applying the orthogonality condition, double right-shift on first filters is conducted. This process yields filters configuration which is shown in Figure 5.

According to Figure 3, double-shift orthogonality gives one relation:

$$\bar{h}_1 h_{-1} + \bar{h}_2 h_0 = \left(\frac{1}{2\sqrt{2}} \times \frac{1}{2\sqrt{2}} \right) + \left(\frac{1-a}{4\sqrt{2}} \times \frac{1}{\sqrt{2}} \right) = 0 \tag{13}$$

Solution for Eq. (13) is that $a = 2$, therefore the 3/5 biorthogonal filters coefficients are:

$$\bar{h} = \left(\bar{h}_{-2}, \bar{h}_{-1}, \bar{h}_0, \bar{h}_1, \bar{h}_2 \right) = \left(\frac{-1}{4\sqrt{2}}, \frac{1}{2\sqrt{2}}, \frac{3}{2\sqrt{2}}, \frac{1}{2\sqrt{2}}, \frac{-1}{4\sqrt{2}} \right) \tag{14}$$

It can be shown that the normality condition is satisfied. That is, it can be seen, with no shift, multiplying the filter coefficients in corresponding position, and then summing all multiplied coefficients, the result is 1. This result can be explained easily in Figure 4.

$$\begin{matrix} 0 & \frac{1}{2\sqrt{2}} & \frac{1}{\sqrt{2}} & \frac{1}{2\sqrt{2}} & 0 \\ \frac{-1}{4\sqrt{2}} & \frac{1}{2\sqrt{2}} & \frac{3}{2\sqrt{2}} & \frac{1}{2\sqrt{2}} & \frac{-1}{4\sqrt{2}} \end{matrix}$$

Figure 4. Filters coefficient of 3/5 biorthogonal.

Table 1. Euclidean Distance and MSE Between Reconstructed Images and the Original Images.

No.	Wavelet Types	CASIA Database Image		Irdosoft 4.0 Camera Image	
		Euclidean Distance	MSE	Euclidean Distance	MSE
1	Haar	1.1567×10^{-13}	9.5565×10^{-28}	9.5329×10^{-14}	8.2615×10^{-28}
2	db5	1.0832×10^{-10}	8.3811×10^{-22}	9.7398×10^{-11}	8.6239×10^{-22}
3	coif3	7.1285×10^{-11}	3.6297×10^{-22}	5.7406×10^{-11}	2.9959×10^{-22}
4	sym4	5.8662×10^{-11}	2.4580×10^{-22}	4.2551×10^{-11}	1.6460×10^{-22}
5	bior2.4	6.0709×10^{-14}	2.6325×10^{-28}	6.5122×10^{-14}	3.8554×10^{-28}
6	bior3.5*)	1.1654×10^{-13}	1.3581×10^{-27}	1.3482×10^{-13}	1.6523×10^{-27}

*New 3/5 Biorthogonal Wavelet

Applying the cascade algorithm up to 20 iterations to form both scaling and wavelet functions for both decomposition and reconstruction can be shown in Figure 6. From this figure, we can see that (a) we can construct plots of both scaling and wavelet functions for decomposition and reconstruction, respectively, which converge to fixed points; (b) biorthogonal wavelet bases maintain the symmetrical property for wavelets and scaling functions by relaxing the orthogonality constraint.

4 Results and discussion

4.1 Image reconstruction tests using MSE and Euclidean distance

The orthogonal/biorthogonal wavelet types, i.e., Haar, db5, coif3, sym4, and bior2.4 which used in former research together with the 3/5 biorthogonal wavelet designed, were tested. Some tests were conducted to measure the performance based on MSE and Euclidean distance between reconstructed images of decomposized iris images and their original input images. In these tests, an unwrapped iris image from CASIA database, as well as from an image captured by Irdosoft 4.0 camera, as we can seen in Figure 5. As we can seen in Table 1, the new 3/5 biorthogonal wavelet (bior3.5) has the good result in reconstructing the decomposized iris image, bior3.5 is ranked at third after Haar and bior2.4.

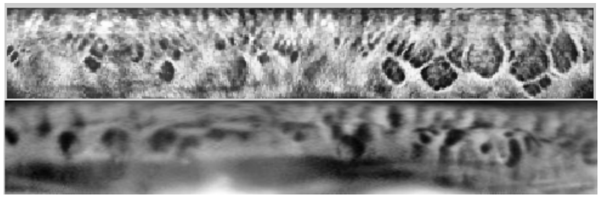

Figure 5. Iris images tested from CASIA (left) and Irdosoft 4.0 (right).

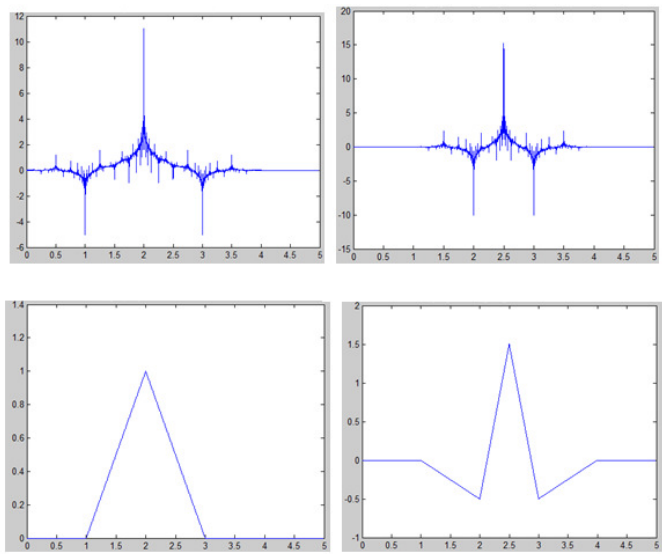

Figure 6. The shapes of scaling function (left) and wavelet function (right) of biorthogonal filter 3/5 for the decomposition (top) and reconstruction (bottom).

4.2 Recognition rate test

We used 30 iris images data from CASIA iris database for recognition rate test. In these tests, we use *d* feature extraction using bior3.5 wavelet and Euclidean distance used for recognition. The recognition rate of the new wavelet bior3.5 with decomposition level 1 is 100%. It also suggests that bior3.5 wavelet is matched to extract the iris images (Figure 6).

5 Conclusions

Some conclusions can be obtained as follows.

1. A new type of wavelet has been found, i.e., bior3.5, which has properties: biorthogonal; filter length for decomposition and reconstruction, respectively, are $N_d = 3$ and $N_r = 5$.

2. The new 3/5 biorthogonal wavelet (bior3.5) has the good result in reconstructing the decomposized image which is captured by Irdosoft 4.0 camera, when compared with other types of wavelet (db5, coif3, and sym4). However, using those measures, bior3.5 is ranked at third after Haar and bior2.4.
3. When applied to CASIA database image, bior3.5 gives the good result compared with three (three) type of wavelets (db5, coif3, and sym4), although it only differs slightly below the bior2.4 which results in best performance, regarding in Euclidean distance and MSE.

Acknowledgment

Authors have to thank to BOPTN 2014 for their financial support for which this research can be done.

References

[1] CASIA-IrisV1, http://biometrics.idealtest.org/

[2] C.S. Burrus, R.A. Gopinath, H. Guo, *Introduction to Wavelets and Wavelet Transforms: A Primer*, Prentice-Hall, Upper Saddle River, New Jersey, 1998.

[3] K.P. Soman, K.I. Ramachandran, N.G. Resmi, *Inside into Wavelets: From Theory to Practice,* 3rd ed., PHI Learning Private Limited, New Delhi, 2010.

[4] R.R. Isnanto, T.S. Widodo, Suhardjo, et al., Wavelet types comparison for extracting iris features based on energy compaction. In: *Proceedings of The 3rd ICSIIT 2012 (International Conference on Soft Computing, Intelligent System, and Information Technology),* Bali, 2012, pp. 88–93.

[5] S. Mallat, *A Wavelet Tour of Signal Processing*, 2nd ed., Academic Press, London, 1999.

[6] N. Nikolaev, A. Gotchev, ECG signal denoising using wavelet domain wiener filtering. In: *Proceeding of the European Association for Signal and Image Processing (EURASIP)*, 2000.

[7] R.R. Isnanto, Suhardjo, A. Susanto, Constructing new biorthogonal wavelet type which matched for extracting the iris image features. *Journal of Physics: Conference Series,* **423(012020)**, 2013, http://iopscience.iop.org/ 1742-6596/423/1/012020.